Progress In Electromagnetics Research C, Vol. 120, 145–157, 2022

Effect of Temperature on the Properties of Omnidirectional Mirror one Dimensional Photonic Crystal

Olfa Nasri[1, *], Jihene Zaghdoudi[1, 2], and Mounir Kanzari[1, 3]

Abstract—In this work, we present numerical results regarding the effects of temperature on the omnidirectional photonic band gap (OPBG) of ternary 1DPC containing metal (Ag) layer or graphene layer. By periodically introducing layer metal (Ag) or graphene into 1DPC, the width of OPBG has been increased. As the temperature increases, the photonic band gap of the OPBG becomes wider. Compared to the conventional OPBG in 1DPC containing Ag, the OPBG in ternary 1DPC containing graphene with temperature $T = 1000°\text{K}$ is greatly broadened by 2.04 times. The theoretical basis of our study adopts the transfer matrix method TMM. In fact, these broad omnidirectional and thermally tunable OPBGs will offer many prospects for omnidirectional mirrors, temperature sensing device, optical filters, polarizer, and other optical devices.

1. INTRODUCTION

Photonic crystals (PCs) are a novel class of artificially fabricated periodic structures that have the ability to control, manipulate, and guide the propagation of electromagnetic waves in contrast with conventional structures [1]. PCs can inhibit the propagation of light, allow it only in certain frequency regions, or localize light in specific spatial regions. These regions are called photonic band gaps (PBGs), and they have been a crucial topic in optical physics over the past two decades [2]. Also, these PCs lead to various potential applications in optoelectronics and optical communication of photonic crystal based devices [1, 3–8]. Photonic crystals can be synthesized in one, two, and three dimensions (1-D, 2-D, and 3-D) with dielectric or/and metallic materials [9–12]. The omnidirectional band gap (OBG) can reflect all incident light independent of the incidence angle, within a certain wavelength range [13–27]. Omnidirectional properties have been shown using one-dimensional photonic crystals [12, 13], clad superlattice structures [14, 15], multilayered heterostructure [16, 17], and ternary photonic band gap materials [18, 19].

Since the first works by Yablonovitch and John (1987) [28, 29], the number of research (in theory and experiment) papers regarding PCs kept increasing, and has greatly attracted the attention of the scientific community for its technological applications, such as reflecting mirrors, filter, photonic crystal waveguide, splitters, resonant cavities, Fabry Perot resonator, and coupler.

On the other hand, many researches have paid close attention to utilizing dispersive or dissipative medium to form tunable PCs such as metal [30], semiconductor [31], superconductor [32], and graphene [33]. Obviously, the possibility of affecting the photonic band gap (PBG) using an external agent such as temperature opens a new perspective in scientific research and technological applications. Temperature tuning can be achieved by thermal expansion and thermo-optical effects in the constituent material of the structure [34, 35].

Received 5 March 2022, Accepted 7 May 2022, Scheduled 22 May 2022

* Corresponding author: Olfa Nasri (olfanasri86@gmail.com).

[1] Laboratoire de Photovoltaïque et Matériaux Semi-conducteurs (LPMS), Ecole Nationale d'Ingénieurs de Tunis (ENIT), Université de Tunis El Manar, BP 37, le Belvédère, Tunis 1002, Tunisie. [2] Institut Supérieur de Technologies de l'Environnement de l'Urbanisme et du Bâtiment (ISTEUB), Université de Carthage, rue de l'Artisanat Charguia 2, Tunis 2035, Tunisie. [3] Institut Préparatoire aux Etudes d'Ingénieurs de Tunis (IPEIT), Université de Tunis, 2, Rue Jawaher Lel Nehru, Montfleury 1089, Tunisie.

In the present work, we study the effect of temperature on photonic band gaps of ternary one dimensional photonic crystal (ternary 1DPC) of structures ($Si/SiO_2/Ag$) and (Si/SiO_2/Graphene). Thus, we have chosen the temperature range from 300°K to 1000°K in this work. Since omnidirectional reflection (ODR) is an important parameter, the dependence of photonic band gap with incident angle has been included in this study.

2. THEORY MODEL AND FORMALISM

The method used to extract the intensity of the electric field is based on the transfer matrix method (TMM), which is one of the most effective methods to analyze the transmission properties of the one dimensional photonic crystals. Based on Abeles method, in terms of the forward $E+$ and backward $E-$ propagation electric fields, which were introduced to calculate the reflection and transmission [36], we show the amplitude of the incident electric wave E_0^+ and the reflected electric wave E_0^-, as a function of both the transmitted and reflected electric filed amplitudes after m layers. E_{m+1}^+ is expressed as the following matrix for stratified films within m layers [37, 38]:

$$\left(\frac{E_0^+}{E_0^-}\right) = \frac{C_1C_2C_3...C_{m+1}}{t_1t_2t_3...t_{m+1}}\left(\frac{E_{m+1}^+}{E_{m+1}^-}\right), \tag{1}$$

Here, C_m is the transfer matrix whose elements are given by [39]:

$$\begin{pmatrix} \dfrac{e^{-i\varphi_m}}{t_m} & \dfrac{r_m e^{i\varphi_m}}{t_m} \\ \dfrac{r_m e^{-i\varphi_m}}{t_m} & \dfrac{e^{i\varphi_m}}{t_m} \end{pmatrix} \tag{2}$$

where t_m and r_m are the Fresnel transmission and reflection coefficients expressed as follows by using the complex refractive index $\hat{n}_m = n_m + ik_m$ and refractive angle θ_m [40].

For TM mode (parallel polarization (P)) [41]:

$$r_{mp} = \frac{\hat{n}_{m-1}\cos\theta_m - \hat{n}_m\cos\theta_{m-1}}{\hat{n}_{m-1}\cos\theta_m + \hat{n}_m\cos\theta_{m-1}}; \quad t_{mp} = \frac{2\hat{n}_{m-1}\cos\theta_{m-1}}{\hat{n}_{m-1}\cos\theta_m + \hat{n}_m\cos\theta_{m-1}}. \tag{3}$$

Moreover, for TE mode (perpendicular polarization (S)) [42]:

$$r_{ms} = \frac{\hat{n}_{m-1}\cos\theta_{m-1} - \hat{n}_m\cos\theta_m}{\hat{n}_{m-1}\cos\theta_{m-1} + \hat{n}_m\cos\theta_m}; \quad t_{ms} = \frac{\hat{n}_{m-1}\cos\theta_{m-1}}{\hat{n}_{m-1}\cos\theta_{m-1} + \hat{n}_m\cos\theta_m} \tag{4}$$

For polarizations TE and TM, the transmittance T and reflectance R are given by the following system [42]:

$$\begin{aligned} T_s &= \mathrm{Re}\left(\frac{\hat{n}_{m+1}\cos\theta_{m+1}}{\hat{n}_0\cos\theta_0}\right)|t_{ms}|^2; \quad T_p = \mathrm{Re}\left(\frac{\hat{n}_{m+1}\cos\theta_{m+1}}{\hat{n}_0\cos\theta_0}\right)|t_{mp}|^2. \\ R &= |r_m|^2. \end{aligned} \tag{5}$$

where φ_m represents the phase variation between the layer (m) and the next one ($m+1$) which is expressed by [43]:

$$\varphi_0 = 0; \quad \varphi_m = \frac{2\pi}{\lambda}n_m d_m. \tag{6}$$

where λ defines the wavelength of the incident light in the vacuum, and d_m, n_m, and θ_m are the refractive index, thickness, and refractive angle of the mth layer, respectively.

3. RESULTS AND DISCUSSION

We consider a ternary one dimensional photonic crystal (ternary 1DPC) structure with the arrangement of $(HLC)^N$, as schematically depicted in Figure 1. The periodic structure is a ternary 1DPC composed

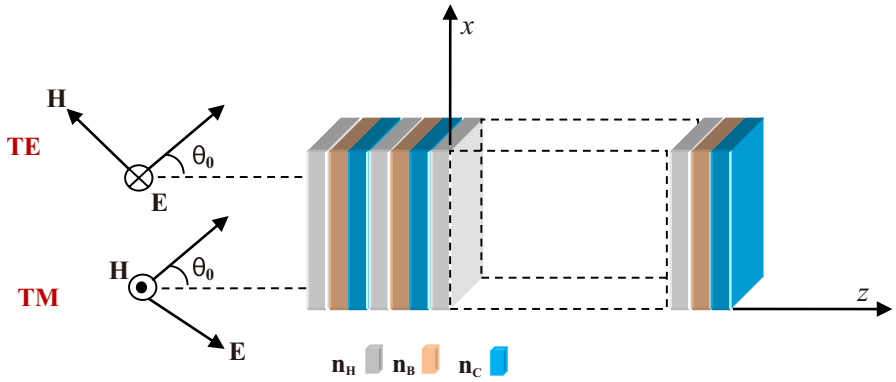

Figure 1. Schematic of the chosen one-dimensional ternary photonic crystal $(\mathrm{HBC})^N$.

of three materials: Si as high refractive index material (H) with refractive index n_H and thickness d_H, the SiO_2 as low refractive index materiel (L) with refractive index n_L and thickness d_L. C is the defect material having a refractive index n_C and thickness d_C, and the structure has form $(\mathrm{HLC})^{20}$. The reference wavelength λ_0 is taken equal to 500 nm. It is assumed that the incident media is air $(n_0 = 1)$. Light is incident on the multilayer at an angle θ_0.

The structure is made of quarter-wave layers which are assumed to satisfy the Bragg condition:

$$n_H d_H = n_B d_B = \frac{\lambda_0}{4}, \tag{7}$$

To study the variation with temperature of the thickness and refractive index of the materials Si and SiO_2, let us simultaneously consider the thermo-optical and thermal expansion effects. As shown, the thickness and refractive index of dielectric layers can be changed due to the thermal-expansion and thermo-optical effects. In certain temperature range, the thermal-expansion effect can be described as [32, 34].

$$d\,(T) = d_0\,(1 + \alpha \Delta T)\,. \tag{8}$$

Here α is the thermal expansion coefficient, and ΔT is the temperature deviation. d and d_0 are the thickness of each layer under the actual temperature and room temperature, respectively. According to the thermo-optical effect, the relation between the temperature and refractive index can be written as [32, 34].

$$n\,(T) = n_0\,(1 + \beta \Delta T)\,. \tag{9}$$

where β is the thermo-optic coefficient.

n and n_0 are the refractive indexes of each layer under the actual temperature and room temperature, respectively. The values of the thermo-optical coefficient, thermal expansion coefficient, and refractive index for Si and SiO_2 are given in Table 1 [10].

Table 1. The characteristics of the constituent materials of 1DPC.

Materials	Refractive index	Thermo-optic coefficient (K^{-1})	Thermal expansion coefficient (K^{-1})	
H (Si)	3.3	1.86×10^{-4}	0.5×10^{-6}	**[10]**
B (SiO_2)	1.45	1×10^{-5}	5.5×10^{-7}	**[10]**

3.1. The Optical Response of Structure with Metal Defect

In this part, we choose metal Ag as a defect material and explore the optical response of the structure ($Si/SiO_2/Ag$). For simplicity, we start by adopting the Drude model metal [44–47]:

$$\varepsilon_m = 1 - \frac{\omega_p^2}{\omega\left(\omega + i\omega_c\left(T\right)\right)}, \tag{10}$$

where m represents the metal, λ the wavelength, ω_c the electron collision frequency, ω_p the plasma frequency, and ω the angular frequency.

The temperature dependence of plasma is very small due to volume expansion, and consequently, ω_p can be approximately a constant. The silver dielectric function can be approximately modeled using $\omega_p = 8.28\,\text{eV}$ [48, 49].

Therefore, the collision frequency is given by [48, 49]:

$$\omega_c\left(T\right) = \left(\frac{0.048}{300^{1.3}}\right) T^{1.3}, \tag{11}$$

So we obtain the refractive index of the material [48, 49]:

$$n_m = \sqrt{\varepsilon_m}. \tag{12}$$

The plot of the refractive index as the function of wavelength and temperature is shown in Figure 2. From this figure, it is clear that the refractive index of Si layers increases with temperature more than that of SiO_2. The increase of the contrast affects the photonic band gap (PBG) by increasing its width. So we can conclude that the photonic band gaps can be shifted as a function of temperature due to thermo-optic effects as displayed in Figure 3.

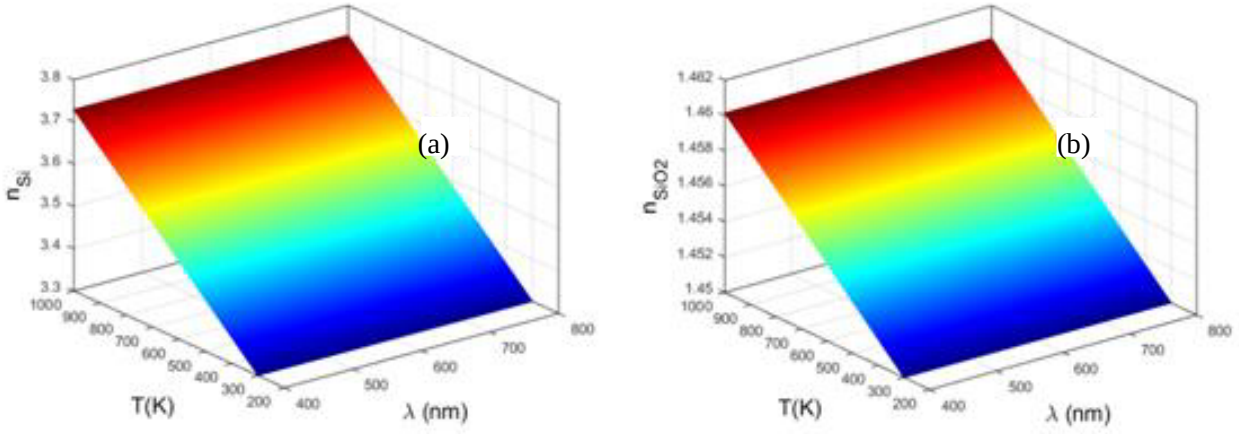

Figure 2. Variation of refractive index as a function of λ and T for tow materials, (a) Si and (b) SiO_2.

In Figure 4, we present the variation of the center (a) and the width at middle half (b) of the PBG as a function of the temperature of the studied structure. It is clear that by increasing the temperature the band gaps shift slightly towards the longer wavelengths region, and it has a linear dependence on the temperature (Figure 4(a)). This can be explained by the variation of the refractive index of Ag layer with temperature more than the variation of refractive index of both Si and SiO_2 layers with temperature.

In addition, it is found that the width at middle half of the PBG increases (Figure 4(b)) and reaches $\Delta\lambda_{\text{PBG}} = 171,2\,\text{nm}$ for $T = 1000°\text{K}$.

Now we fix the temperature to $T = 300°\text{K}$, and we vary the incident angle in order to study the effect of the polarization. The optical response is represented in Figure 5 for TM and TE modes. We note that the TE polarization bandwidth gets broader as the incident angle θ increases, whereas the TM polarization bandwidth becomes narrower.

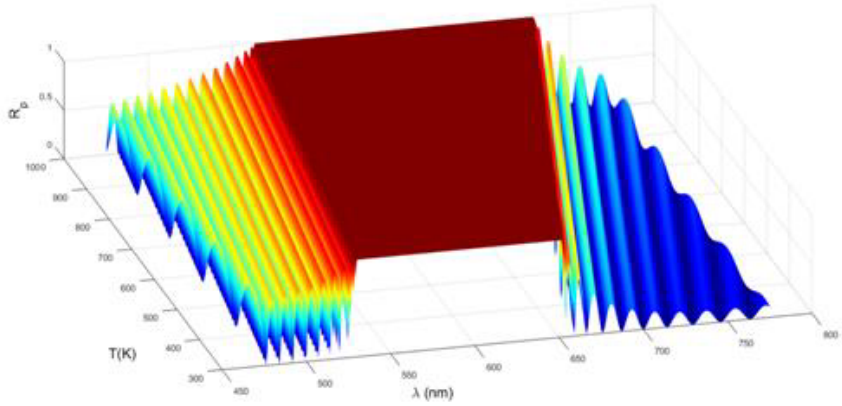

Figure 3. Reflectance spectrum at normal incidence of the structure ($Si/SiO_2/Ag$) as a function of λ and T at normal incidence.

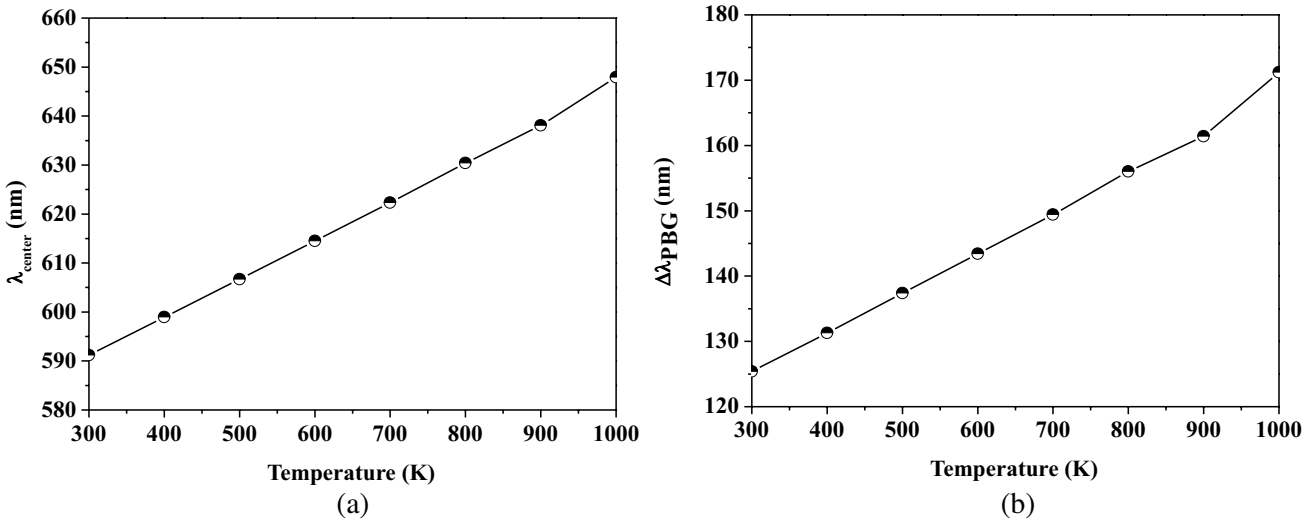

Figure 4. Variation of (a) the center wavelength λ_{center} of the PBG and (b) the width at middle half $\Delta\lambda_{\text{PBG}}$ as a function of T at normal incidence.

For analyzing the incident angle effect more, we show in Figure 6 the variation of the two edges of the photonic band gap ($\lambda_{\text{long}}(\theta_0)$ and $\lambda_{\text{short}}(\theta_0)$) in both TM and TE polarized lights. From this figure the broadness of the omnidirectional photonic band gap (OPBG) is equal to 31 nm for $T = 300°\text{K}$.

Indeed, this work concerns the study of the effect of temperature. Therefore, we vary the temperature in the range 300°K–1000°K, and every time we extract the width of the omnidirectional photonic band gap (OPBG). Figure 7 shows the obtained results data as a 2D curve.

By analyzing this figure, we conclude that the OPBG increases rapidly with temperature from 31 nm to 70,5 nm as shown in Figure 8.

Compared to the conventional OPBG at $T = 300°\text{K}$, the OPBG at $T = 1000°\text{K}$ is greatly broadened by 414 times. According to the preceding results, one can consider that our structure is suitable for different applications as a temperature sensing device, narrow band optical filter, wavelength division demultiplexer, tunable omnidirectional reflector, and in many optical systems. In order to recognize the effect of the nature of material, we study the optical response of the structure when we change the metal by the graphene.

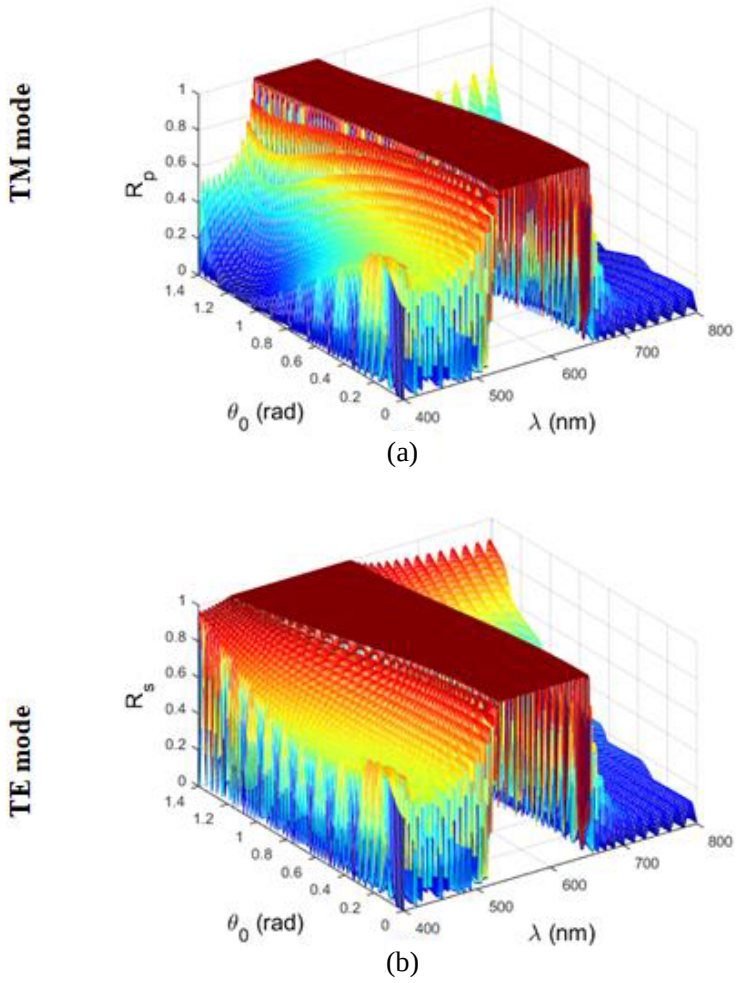

Figure 5. Reflectance spectrum of the structure ($Si/SiO_2/Ag$) as a function of θ_0 and λ for both polarization (a) TM: and (b) TE: for $T = 300°K$.

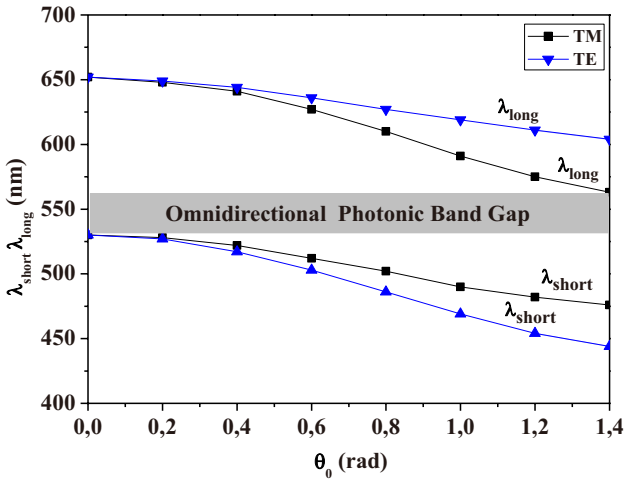

Figure 6. Reflection band shift of structure ($Si/SiO_2/Ag$) as a function of incident angle at $T = 300°K$.

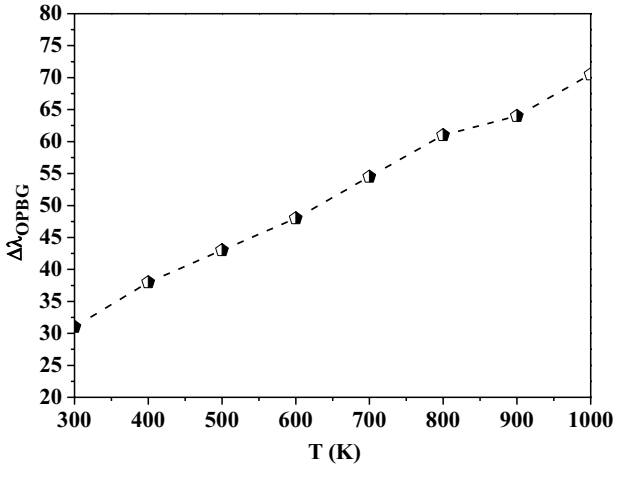

Figure 7. Variation of omnidirectional photonic band gap ($\Delta\lambda_{OPBG}$) of structure ($Si/SiO_2/Ag$) as a function of temperature (T).

3.2. The Optical Response of Structure with Graphene Defect

The studied structure in this part is (Si/SiO_2/Graphene). It is known that the graphene can be characterized by a surface conductivity that can be calculated using the Kubo formula [50–53] which is expressed as:

$$\sigma_g(\omega, \mu_c, \Gamma, T) = \sigma_{\text{intra}} + \sigma_{\text{inter}}, \tag{13}$$

with

$$\sigma_{\text{intra}} = -j\frac{e^2 k_B T}{\pi\hbar^2(\omega - 2j\Gamma)}\left\{\frac{\mu_c}{k_B T} + 2\ln\left(\exp\left(-\frac{\mu_c}{k_B T}\right) + 1\right)\right\}, \tag{14}$$

and

$$\sigma_{\text{inter}} = -j\frac{e^2}{4\pi\hbar}\ln\left\{\frac{2|\mu_c| - (\omega - 2j\Gamma)\hbar}{2|\mu_c| + (\omega - 2j\Gamma)\hbar}\right\}, \tag{15}$$

Here, σ_{intra}, σ_{inter}, ω, e, Γ, and μ_c are respectively the intra-band, inter-band, angular frequency, the charge of an electron, a scattering rate, and the chemical potential of the graphene. In addition, T, k_B, and $\hbar = h/2\pi$ are the Kelvin temperature, the Boltzmann's constant, and the reduced Plank's constant, respectively.

It is known that the surface conductivity of graphene depends predominantly on intraband transitions and interband transitions that are negligible [54]. Therefore, the graphene conductivity

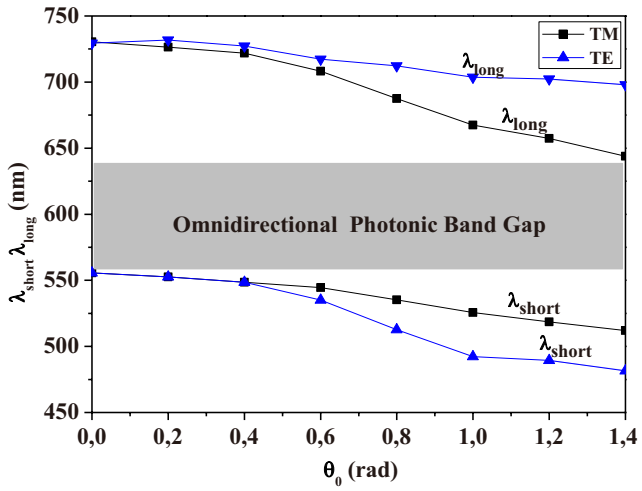

Figure 8. Reflection band shift of structure (Si/SiO_2/Ag) as a function of incident angle at $T = 1000°K$.

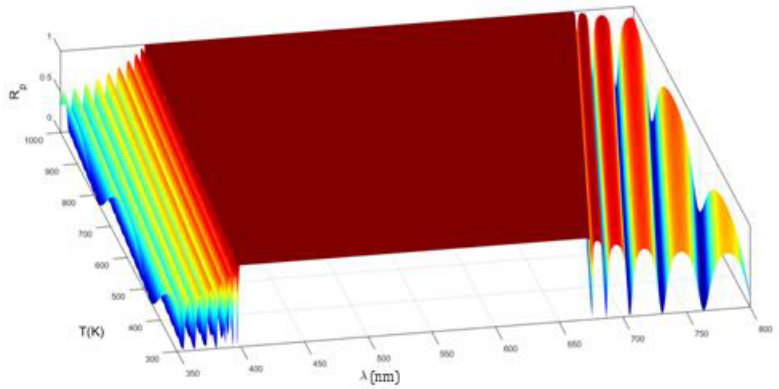

Figure 9. Reflectance spectrum at normal incidence of the structure (Si/SiO_2/Graphene) as a function of λ and T at normal incidence.

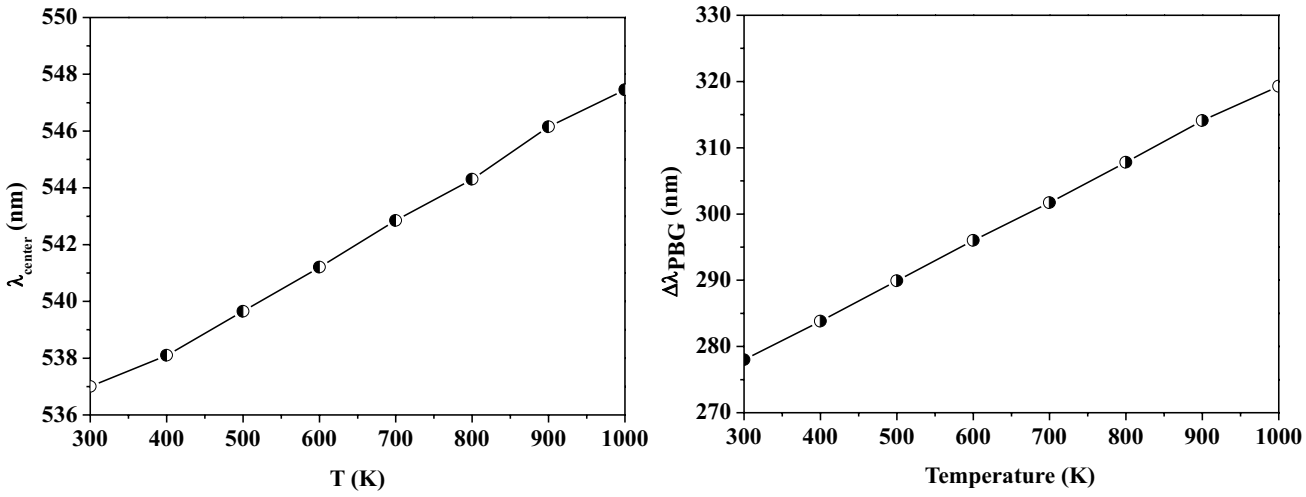

Figure 10. Variation of (a) the center wavelength λ_{center} of the PBG and (b) the width at middle half $\Delta\lambda_{\text{PBG}}$ as a function of temperature (T) at normal incidence.

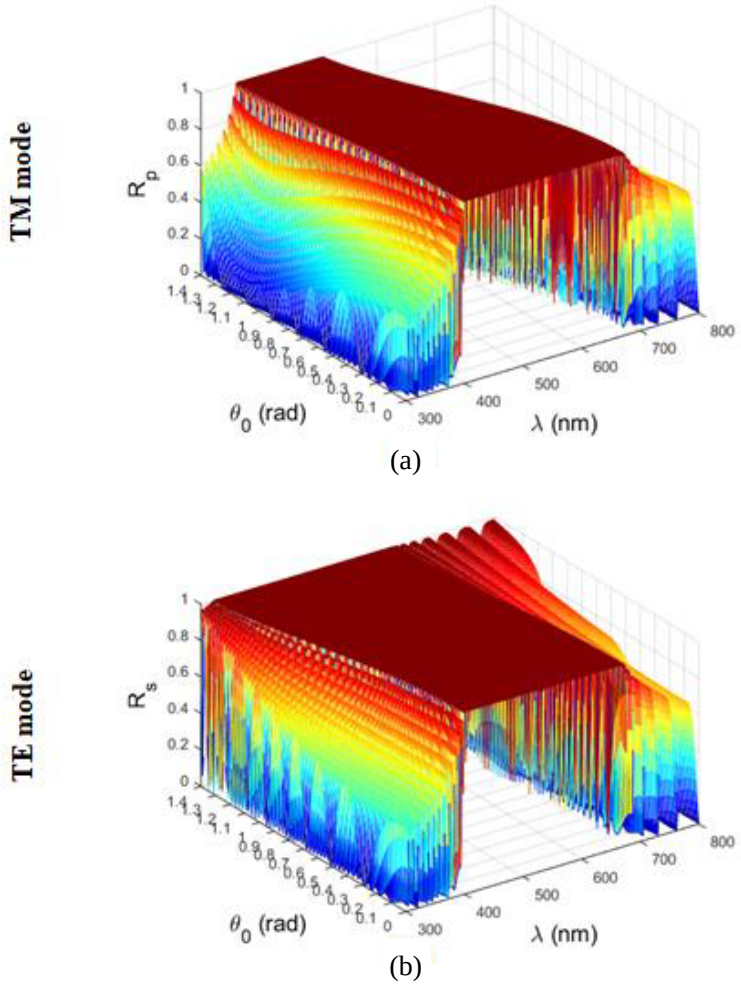

Figure 11. Reflection spectrum of the structure (Si/SiO_2/Graphene) as function of θ_0 and λ for both polarization (a) TM: and (b) TE: for $T = 300°K$.

formula can be simplified as [53, 54]:

$$\sigma_g = \frac{\sigma_0}{2\Gamma + j\omega}, \tag{16}$$

$$\sigma_0 = \frac{e^2 k_B T}{\pi\hbar^2}\left[\frac{\mu_c}{k_B T} + 2\ln\left(\exp\left(-\frac{\mu_c}{k_B T}\right)+1\right)\right]. \tag{17}$$

The permittivity of graphene ε_g can be derived from the precedent equations, and it is given by [53, 54]:

$$\varepsilon_g = 1 - \frac{j\sigma_g}{\omega\varepsilon_0 d} = 1 - \frac{\sigma_0}{(\omega^2 - 2j\Gamma)d\varepsilon_0}. \tag{18}$$

We present in Figure 9 the variation of the reflectance of structure (Si/SiO_2/Graphene) versus temperature and wavelength at normal incidence.

We note that when the temperature increases, the bandwidth at half height increases too (Figure 10(b)), and the center of the band gaps (Figure 10(a)) shifts slightly towards the high wavelengths regions because the rate of change in the refractive index of the graphene layer with temperature is more than that of both Si and SiO_2 layers with temperature.

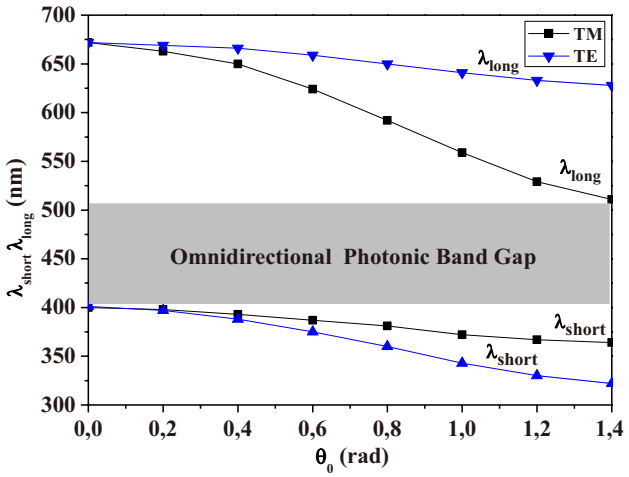

Figure 12. Reflection band shift of the structure (Si/SiO_2/Graphene) as a function of incident angle for $T = 300°K$.

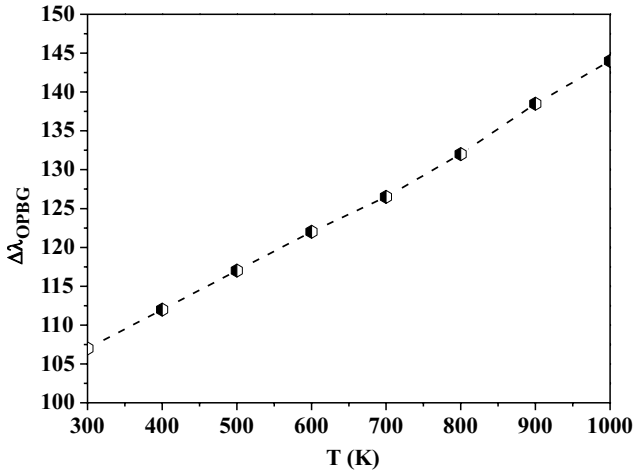

Figure 13. Variation of omnidirectional photonic band gap ($\Delta\lambda_{OPBG}$) of the structure (Si/SiO_2/Graphene) as function of temperature.

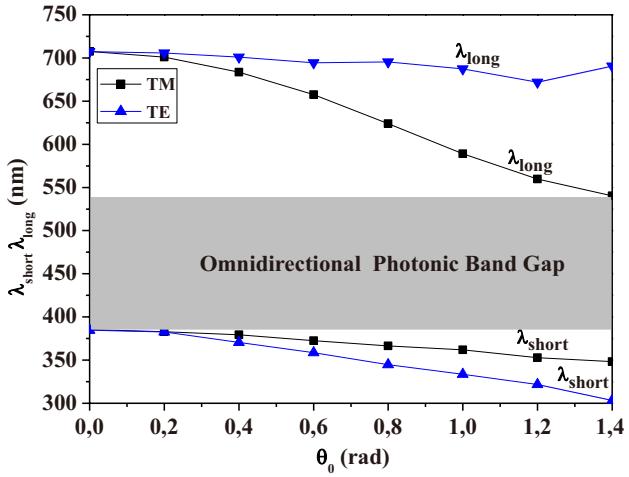

Figure 14. Reflection band shift of the structure (Si/SiO_2/Graphene) as a function of incident angle for $T = 1000°K$.

In Figure 11, we presents the reflections R_p and R_s of the structure (Si/SiO_2/Graphene) versus wavelength λ and incident angle θ_0 for the temperature $T = 300°K$.

For the selected value of temperature (see Figure 11), the TE polarization bandwidth gets broader as the incident angle θ_0 increases, whereas the TM polarization bandwidth becomes narrower. We obtain a large OPBG for both polarizations TM and TE (Figure 12), equal to 107 nm for $T = 300°K$. This result is almost the double of that obtained when we incorporate the metal.

To appreciate the effect of the temperature on the OPBG in 1DPC containing graphene at oblique incidence, we present in Figure 13 the variation of the width of the OPBG versus temperature for $T \in [300, 1000]°K$. We can conclude that graphene heating improves the width of the OPBG.

For both polarizations, the OPBG increases quickly with temperature from 107 nm at $T = 300°K$ to 144 nm for $T = 1000°K$ as shown in Figure 14.

Compared to the conventional OPBG at $T = 300°K$, the OPBG at $T = 1000°K$ is greatly broadened by 1.34 times.

These results may be of interest to promote various applications based on tunable OPBG.

4. CONCLUSION

In summary, we have designed a new type of broad omnidirectional and thermally tunable PBGs in ternary 1DPC containing a metal (Ag) or a graphene. The incident angle and temperature dependence of these OPBGs have been investigated. We found that the width of these OPBGs can be enhanced with temperature. It has been found that the width of OPBG in ternary 1DPC containing a metal is about 31 nm at $T = 300°K$ whereas for $T = 1000°K$ the OPBG is about 70,5 nm. In the case of the graphene, the width of OPBG is about 107 nm for $T = 300$ K and 144 nm for $T = 1000°K$. Such broad omnidirectional and thermally tunable OPBGs will offer many prospects for omnidirectional mirrors, temperature sensing device, optical filters, polarizer, and other optical devices in the optical communications domains. Further calculations are planned to be enhanced.

REFERENCES

1. Joannopoulos, J. D., S. G. Johnson, J. N. Winn, and R. D. Meade, *Photonic Crystals: Molding the Flow of Light*, Princeton University Press, Princeton, New Jersey, 2008.
2. Arismar Cerqueira, S., "Recent progress and novel applications of photonic crystal fibers," *Rep. Prog. Phys.*, Vol. 73, No. 2, 024401, 2010, doi: 10.1088/0034-4885/73/2/024401.
3. Najafgholinezhad, S. and S. Olyaee, "A photonic crystal biosensor with temperature dependency investigation of micro-cavity resonator," *Optik*, Vol. 125, No. 21, 6562–6565, Nov. 2014, doi: 10.1016/j.ijleo.2014.08.043.
4. Liu, D., L. Chen, D. Cao, and F. Liu, "Terahertz metallic photonic crystals integrated with dielectric waveguides," *Opt. Commun.*, Vol. 475, 126197, 2020, doi: 10.1016/j.optcom.2020.126197.
5. Kumar, A., V. Kumar, A. Nautiyal, Kh. S. Singh, and S. P. Ojha, "Optical switch based on nonlinear one dimensional photonic band gap material," *Optik*, Vol. 145, 473–478, Sept. 2017, doi: 10.1016/j.ijleo.2017.07.062.
6. Zheng, Q.-R., Y.-Q. Fu, and N.-C. Yuan, "Characteristics of planar PBG structures with a cover layer," *Journal of Electromagnetic Waves and Applications*, Vol. 20, No. 11, 1439–1453, 2006.
7. Ozbay, E., B. Temelkuran, and M. Bayindir, "Microwave applications of photonic crystals," *Progress In Electromagnetics Research*, Vol. 41, 185–209, 2003.
8. Hao, K., et al., "Design of one-dimensional composite photonic crystal with high infrared reflectivity and low microwave reflectivity," *Optik*, Vol. 216, 164794, 2020, doi: 10.1016/j.ijleo.2020.164794.
9. Zamudio-Lara, A., et al., "Characterization of metal-dielectric photonic crystals," *Opt. Mater.*, Vol. 29, No. 1, 60–64, Oct. 2006, doi: 10.1016/j.optmat.2006.03.026.
10. Alejo-Molina, A., D. L. Romero-Antequera, and J. J. Sánchez-Mondragón, "Localization and characterization of the metallic band gaps in a ternary metallo-dielectric photonic crystal," *Opt. Commun.*, Vol. 312, 168–174, 2014, doi: 10.1016/j.optcom.2013.09.021.

11. Jannesari, R., C. Ranacher, C. Consani, T. Grille, and B. Jakoby, "Sensitivity optimization of a photonic crystal ring resonator for gas sensing applications," *Sens. Actuators Phys.*, Vol. 264, 347–351, Sept. 2017, doi: 10.1016/j.sna.2017.08.017.
12. Barvestani, J., "Omnidirectional narrow bandpass filters based on one-dimensional superconductor-dielectric photonic crystal heterostructors," *Phys. B Condens. Matter*, Vol. 457, 218–224, 2015, doi: 10.1016/j.physb.2014.10.019.
13. Wang, X., et al., "Enlargement of omnidirectional total reflection frequency range in one-dimensional photonic crystals by using photonic heterostructures," *Appl. Phys. Lett.*, Vol. 80, No. 23, 4291–4293, 2002, doi: 10.1063/1.1484547.
14. Wang, Z., C. Guo, and W. Jiang, "Large mode area OmniGuide fiber with superconductor-dielectric periodic multilayers cladding," *Optik*, Vol. 125, No. 22, 6789–6792, Nov. 2014, doi: 10.1016/j.ijleo.2014.08.079.
15. Bria, D., B. Djafari-Rouhani, E. H. El Boudouti, A. Mir, A. Akjouj, and A. Nougaoui, "Omnidirectional optical mirror in a cladded-superlattice structure," *J. Appl. Phys.*, Vol. 91, No. 5, 2569–2572, 2002, doi: 10.1063/1.1433188.
16. Srivastava, R., S. Pati, and S. P. Ojha, "Enhancement of omnidirectional reflection in photonic crystal heterostructures," *Progress In Electromagnetics Research B*, Vol. 1, 197–208, 2008.
17. Doghmosh, N., S. A. Taya, A. Upadhyay, M. M. Olaimat, and I. Colak, "Enhancement of optical visible wavelength region selective reflector for photovoltaic cell applications using a ternary photonic crystal," *Optik*, Vol. 243, 167491, Oct. 2021, doi: 10.1016/j.ijleo.2021.167491.
18. Castillo-Gallardo, V., L. E. Puente-Díaz, D. Ariza-Flores, H. Pérez-Aguilar, W. L. Mochán, and V. Agarwal, "Optimization of wide-band quasi-omnidirectional 1-D photonic structures," *Opt. Mater.*, Vol. 117, 111202, 2021, doi: 10.1016/j.optmat.2021.111202.
19. Xi, J.-Q., et al., "Omnidirectional reflector using nanoporous SiO_2 as a low-refractive-index material," *Opt. Lett.*, Vol. 30, No. 12, 1518, 2005, doi: 10.1364/OL.30.001518.
20. Nutku, F. and S. Gökşin, "Comparison of omnidirectional reflectivity of quasi-periodic dielectric multilayers," *Optik*, Vol. 228, 166220, 2021, doi: 10.1016/j.ijleo.2020.166220.
21. Awasthi, S. K., U. Malaviya, and S. P. Ojha, "Enhancement of omnidirectional total-reflection wavelength range by using one-dimensional ternary photonic bandgap material," *J. Opt. Soc. Am. B*, Vol. 23, No. 12, 2566, 2006, doi: 10.1364/JOSAB.23.002566.
22. Zhang, H.-F., J.-P. Zheng, and Y. Lin, "Enhancement of omnidirectional photonic band gaps in one-dimensional ternary superconductor-dielectric photonic crystals," *Opt. — Int. J. Light Electron Opt.*, Vol. 124, No. 17, 2858–2863, Sept. 2013, doi: 10.1016/j.ijleo.2012.08.060.
23. Temelkuran, B., E. L. Thomas, J. D. Joannopoulos, and Y. Fink, "Low-loss infrared dielectric material system for broadband dual-range omnidirectional reflectivity," *Opt. Lett.*, Vol. 26, No. 17, 1370, Sept. 2001, doi: 10.1364/OL.26.001370.
24. Park, Y., Y.-G. Roh, C.-O. Cho, H. Jeon, M. G. Sung, and J. C. Woo, "GaAs-based near-infrared omnidirectional reflector," *Appl. Phys. Lett.*, Vol. 82, No. 17, 2770–2772, 2003, doi: 10.1063/1.1569045.
25. Lin, W., G. P. Wang, and S. Zhang, "Design and fabrication of omnidirectional reflectors in the visible range," *J. Mod. Opt.*, Vol. 52, No. 8, 1155–1160, 2005, doi: 10.1080/09500340512331327606.
26. Ben Ali, N. and M. Kanzari, "Designing of omni-directional high reflectors by using one-dimensional modified hybrid Fibonacci/Cantor band-gap structures at optical telecommunication wavelength band," *J. Mod. Opt.*, Vol. 57, No. 4, 287–294, 2010, doi: 10.1080/09500340903545289.
27. Deopura, M., C. K. Ullal, B. Temelkuran, and Y. Fink, "Dielectric omnidirectional visible reflector," *Opt. Lett.*, Vol. 26, No. 15, 1197, 2001, doi: 10.1364/OL.26.001197.
28. Yablonovitch, E., "Inhibited spontaneous emission in solid-state physics and electronics," *Phys. Rev. Lett.*, Vol. 58, No. 20, 2059–2062, 1987, doi: 10.1103/PhysRevLett.58.2059.
29. John, S., "Strong localization of photons in certain disordered dielectric superlattices," *Phys. Rev. Lett.*, Vol. 58, No. 23, 2486–2489, 1987, doi: 10.1103/PhysRevLett.58.2486.

30. Gharaati, A. and Z. Zare, "The effect of temperature on one-dimensional nanometallic photonic crystals with coupled defects," *Pramana*, Vol. 88, No. 5, 75, 2017, doi: 10.1007/s12043-017-1380-5.
31. Malik, J. V., et al., "Effect of temperature on photonic band gaps in semiconductor-based one-dimensional photonic crystal," *Adv. Opt. Technol.*, Vol. 2013, 1–8, 2013, doi: 10.1155/2013/798087.
32. Soltani, O., J. Zaghdoudi, and M. Kanzari, "Analysis of transmittance properties in 1D hybrid dielectric photonic crystal containing superconducting thin films," *Phys. B Condens. Matter*, Vol. 538, 62–69, 2018, doi: 10.1016/j.physb.2018.03.017.
33. Wu, F., M. Chen, Z. Chen, and C. Yin, "Omnidirectional terahertz photonic band gap broaden effect in one-dimensional photonic crystal containing few-layer graphene," *Opt. Commun.*, Vol. 490, 126898, 2021, doi: 10.1016/j.optcom.2021.126898.
34. Baraket, Z., J. Zaghdoudi, and M. Kanzari, "Investigation of the 1D symmetrical linear graded superconductor-dielectric photonic crystals and its potential applications as an optimized low temperature sensors," *Opt. Mater.*, Vol. 64, 147–151, 2017, doi: 10.1016/j.optmat.2016.12.005.
35. El-Amassi, D. M., S. A. Taya, and D. Vigneswaran, "Temperature sensor utilizing a ternary photonic crystal with a polymer layer sandwiched between Si and SiO_2 layers," *J. Theor. Appl. Phys.*, Vol. 12, No. 4, 293–298, 2018, doi: 10.1007/s40094-018-0308-x.
36. Abelès, F., "Recherches sur la propagation des ondes électromagnétiques sinusoïdales dans les milieux stratifiés," *Ann. Phys.*, Vol. 12, 706–782, 1950, doi: 10.1051/anphys/195012050706.
37. Abelès, F., "La détermination de l'indice et de l'épaisseur des couches minces transparentes," *J. Phys. Radium*, Vol. 11, No. 7, 310–314, 1950, doi: 10.1051/jphysrad:01950001107031000.
38. Ohta, K. and H. Ishida, "Matrix formalism for calculation of electric field intensity of light in stratified multilayered films," *Appl. Opt.*, Vol. 29, No. 13, 1952, 1990, doi: 10.1364/AO.29.001952.
39. Habli, O., J. Zaghdoudi, and M. Kanzari, "Effect of the nonlinearity on optical properties of one-dimensional photonic crystal," *Progress In Electromagnetics Research M*, Vol. 100, 69–79, 2021.
40. Zaghdoudi, J. and M. Kanzari, "One-dimensional photonic crystal filter using a gradient-index layer," *Optik*, Vol. 160, 189–196, 2018, doi: 10.1016/j.ijleo.2018.01.129.
41. Zaghdoudi, J., M. Kanzari, and B. Rezig, "Design of omnidirectional high reflectors for optical telecommunication bands using the deformed quasiperiodic one-dimensional photonic crystals," *Proceedings of 2005 7th International Conference Transparent Optical Networks, 2005*, Vol. 2, 322–325, Barcelona, Catlonia, Spain, 2005, doi: 10.1109/ICTON.2005.1506163.
42. Trabelsi, Y., N. B. Ali, and M. Kanzari, "Tunable narrowband optical filters using superconductor/dielectric generalized Thue-Morse photonic crystals," *Microelectron. Eng.*, Vol. 213, 41–46, 2019, doi: 10.1016/j.mee.2019.04.016.
43. Mouldi, A. and M. Kanzari, "Design of an omnidirectional mirror using one dimensional photonic crystal with graded geometric layers thicknesses," *Optik*, Vol. 123, No. 2, 125–131, 2012, doi: 10.1016/j.ijleo.2011.03.010.
44. Holstein, T., "Theory of transport phenomena in an electron-phonon gas," *Ann. Phys.*, Vol. 29, No. 3, 410–535, Oct. 1964, doi: 10.1016/0003-4916(64)90008-9.
45. Holstein, T., "Optical and infrared volume absorptivity of metals," *Phys. Rev.*, Vol. 96, No. 2, 535–536, Oct. 1954, doi: 10.1103/PhysRev.96.535.
46. Lawrence, W. E., "Electron-electron scattering in the low-temperature resistivity of the noble metals," *Phys. Rev. B*, Vol. 13, No. 12, 5316–5319, 1976, doi: 10.1103/PhysRevB.13.5316.
47. Chiang, H.-P., P. T. Leung, and W. S. Tse, "Optical properties of composite materials at high temperatures," *Solid State Commun.*, Vol. 101, No. 1, 45–50, 1997, doi: 10.1016/S0038-1098(96)00558-3.
48. Gharaati, A. and Z. Zare, "Modeling of thermal tunable multichannel filter using defective metallic photonic crystals," *Opt. Appl.*, 2017, doi: 10.5277/OA170410.
49. Zare, Z. and A. Gharaati, "Enhancement of transmission in 1D thermal tunable metallic photonic crystal filter with exponential gradation thickness," *Eur. Phys. J. D*, Vol. 74, No. 7, 140, 2020, doi: 10.1140/epjd/e2020-10057-0.

50. Hanson, G. W., "Dyadic Green's functions and guided surface waves for a surface conductivity model of graphene," *J. Appl. Phys.*, Vol. 103, No. 6, 064302, 2008, doi: 10.1063/1.2891452.
51. Li, Y., L. Qi, J. Yu, Z. Chen, Y. Yao, and X. Liu, "One-dimensional multiband terahertz graphene photonic crystal filters," *Opt. Mater. Express*, Vol. 7, No. 4, 1228, 2017, doi: 10.1364/OME.7.001228.
52. Sayem, A. A., Md. M. Rahman, M. R. C. Mahdy, I. Jahangir, and Md. S. Rahman, "Negative refraction with superior transmission in graphene-hexagonal boron nitride (hBN) multilayer hyper crystal," *Sci. Rep.*, Vol. 6, No. 1, 25442, 2016, doi: 10.1038/srep25442.
53. Xie, X., Y.-J. Liu, L. Ju, J.-J. Hao, and H.-W. Yang, "Study on the spectral selectivity of graphene/superconductor photonic crystals at low temperature," *J. Quant. Spectrosc. Radiat. Transf.*, Vol. 230, 81–85, 2019, doi: 10.1016/j.jqsrt.2019.03.014.
54. Xiang, Y., X. Dai, J. Guo, H. Zhang, S. Wen, and D. Tang, "Critical coupling with graphene-based hyperbolic metamaterials," *Sci. Rep.*, Vol. 4, No. 1, 5483, 2015, doi: 10.1038/srep05483.